A98-31682

ICAS-98-6,5,1

AIRCRAFT VORTEX WAKE, FLIGHT SAFETY AND CRISIS OF AIRPORTS

V.V. Vyshinsky
TsAGI, Russia

Abstract

In the framework of computational and experimental methods, the problem is solved on improving airport capacity. For this purpose a two-level aerodynamic wake model was developed as well as models intended for studying the problems of flight dynamics, structural strength and aeroelasticity. The element of stochasticity inherent in the phenomenon under study is incorporated into the combined model through the two last models. The mathematical models are combined into a single structure, which enables their using to assess hazardous situations associated with vortex wake encounters of aircraft, to construct criteria to judge as reliably as possible the severity of the vortex hazard in landing, to determine the relationship between the probability of accidents and main parameters of both leading and following aircraft, weather conditions in the airport area and distances between aircraft, to work out recommendations on timely detection of vortex wakes and pilot actions to execute a vortex avoidance maneuver and on establishing safe-separation standards.

Nomenclature

V_∞	flight speed;
α_∞	angle of attack;
ρ_∞	ambient air density;
G	aircraft weight;
b	wing span;
S	wing area;
c_{av}	S/b
c_{tip}	wing tip chord length;
C_L	lift coefficient;
C_l	rolling moment coefficient;
Γ	velocity circulation;
Γ_0	total circulation: $G/(\rho_\infty \cdot V_\infty \cdot b)$;
Γ_c	turbulent core circulation;
Γ_{tip}	tip vortex circulation;
z_{tip}	lateral position of the tip vortex;
Γ_{flap}	flap vortex circulation;
δ_{flap}	angle of flap deflection;
c_{flap}	flap chord length;
z_{flap}	lateral position of the flap vortex;
$V_{\tau max}$	maximum tangential velocity in the vortex;
b_v	vortex span (for elliptical span circulation distribution $b_v = b \cdot \pi / 4$);
b_{eq}	equivalent vortex span;
r	vortex radius;
r_{tip}	tip vortex radius;
r_{flap}	flap vortex radius;
h_v	vortex axes height above the ground;
V	vortex descent rate $\Gamma/(2\pi b_v)$;
q	standard value of atmospheric turbulence;
λ_{max}	wavelength of the most quickly growing mode;
A_0	initial amplitude of vortex pair oscillation;
φ	angle of the vortex oscillation plane;
ν	frequency of vortex oscillation: $\nu = 2\pi/\lambda$;
t_{CL}	cross-link time;
D_{CL}	cross-link distance;
$\bar{f}$	ratio of the imposed rolling moment to the rolling moment created by ailerons: $\bar{f} = \frac{C_{l\,pert}}{C_{l\,ail}}$;
ΔM	wing root bending moment;
t_{st}	safe separation interval.

Introduction

For pertinent segmentation of the problem under study and weighed accentuation of its constituents, it is very useful to consider actual vortex encounter-related aircraft accidents. As an example, Figure 1 depicts the scenario of a flight accident[1] occurred at Salt Lake City Airport, Utah, on November 10, 1993. The pilot of a four-seat single-engined piston Cessna 182 Skylane high-wing monoplane ($b=10.92$ m, $G_{max}=1.4$ t) was executing a VFR approach to runway R32. The pilot was warned by ATC that he was following an aircraft (it turned out to be a B-757 whose wake is known to consist of very strong and persistent vortices with a high tangential vortex velocity $V_{\tau max} > 100$ m/s) on approach to runway R35. On final approach the Cessna experienced a burble, and then the nose pitched up 90^o and the airplane suddenly rolled 90^o to the right. The pilot immediately put in full-left deflection of rudder and ailerons and full-down elevator in an attempt to level the airplane. Just leveled off, the aircraft crashed short of the threshold of runway R32, veered to the northeast, and came to the rest on the approach end of runway R35. The aircraft was destroyed, the aircraft occupants suffered minor injuries.

It was found that the Cessna crossed the flight path of the B-757 at an altitude of $h=30$ m over the ground, $\Delta t=38$ s (2660 m) after the latter's passage. According to recorded radar data, the flight path of the Cessna was slightly above the flight path of the B-757.

A mathematical simulation of the situation shows that the velocity of the vortices' moving apart near the ground might be V_{cros}=1.5 -2.5 m/s. With no cross wind (a south wind V_{wind}=2.5 m/s was recorded at the landing site), the left vortex of the B-757 would have translated Δz=60-90 m westward. The altitude of the vortex above the ground, without considering vortex buoyancy, may have reached h_v=20-25 m, with allowance made for buoyancy due to the interaction with secondary vorticity, it may have been h_v=50 m. The vortex core diameter according to estimates made in the framework of the vortex wake model[2] may have been about $2r_o$=1.5 m. A slight cross or tail wind having a velocity of V_{wind}=1.5-2.5 m/s (just such a wind was recorded) corresponds to the worst situation[3].

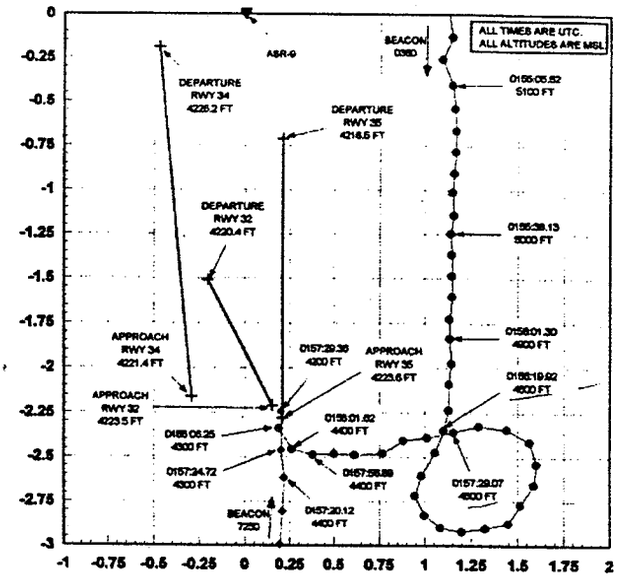

FIGURE 1 - Wake-vortex-related flight accident scenario[1].

Using this example, we would like to accentuate a significant three dimensionality of the flight path, which make the subsequent mutual approach of the aircraft quite possible already after receiving the landing clearance under VFR conditions from the air traffic controller (after this the whole responsibility for flight safety rests with the pilot), as well as the possibility of encountering its own vortex wake as a result of an additional holding of the aircraft by the controller for providing a safe separation interval in landing on the same runway or crossing ones.

The urgency of the problem under study is caused by impossibility in the framework of existing technology to realize the desired growth of air traffic, which leads to economic loses. The necessary commercial fleet growth[4] should be provided with taking into consideration naturally phasing out aircraft due to their aging. The plot presented in Figure 2 allows one to determine the growing percentage of new aircraft, which may be primarily affected by new measures concerning a decrease in safe separation distances (vortex wake attenuation and visualization for leader aircraft and vortex avoidance maneuver and increasing survivability for following aircraft).

Figure 3 and 4 present air traffic data (the number of carried passengers and the number of aircraft movements) for ten major airports of the USA and Europe[5].

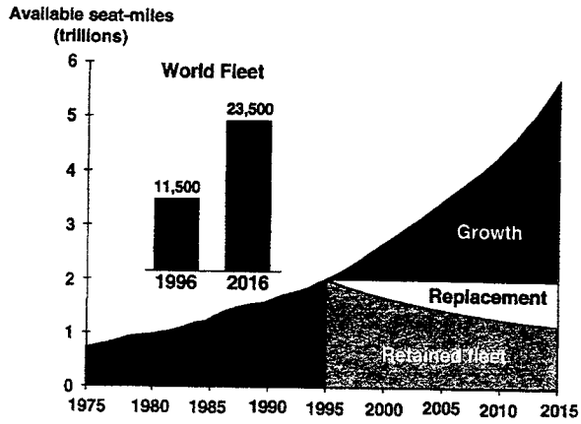

FIGURE 2 – Urgency of the problem under study: a conflict between the required air traffic volume and the limited number of airports.

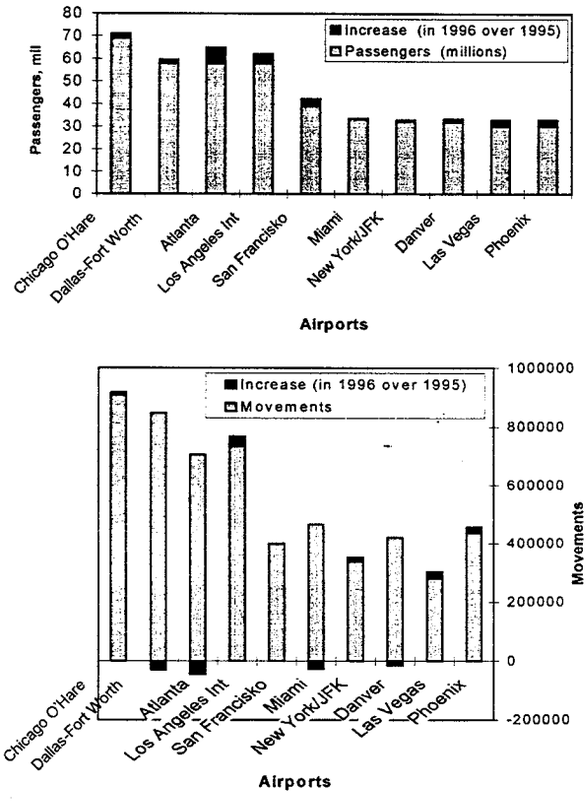

FIGURE 3 – Passenger traffic and aircraft movements at the 10 busiest US airports in 1996.

Two opposite trends can be seen. In the USA, as a result of domination of transcontinental routes in the air transportation system, the growth in the number of passengers takes the lead over the growth in the number of flights. With a general increase in the air traffic volume, in some airports one can see even a decrease in the number

of aircraft movements. On the contrary, in Europe, the air traffic data on relatively saturated hub airports show a trend of aircraft movements' growth exceeding the air traffic growth rate due to introduction of relatively low-capacity passenger aircraft and increase in low-density high-class passenger compartments. In all major airports the growth in aircraft movements is observed.

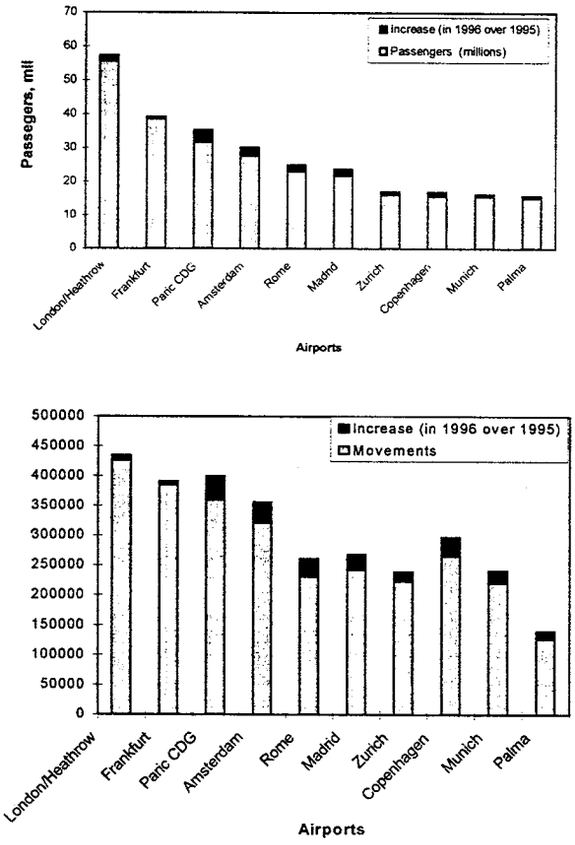

FIGURE 4 – Passenger traffic and aircraft movements at the 10 busiest European airports in 1996.

An analysis of the passenger aircraft market reveals a trend towards sells of relatively low-capacity aircraft, both in the classes of long-range and short-range aircraft. In particular, one can observe superseding 120-seat aircraft DC-9, B-737, and A-319 by more lighter and cheaper 50 – to 70-seat aircraft. The percentage of such aircraft in the USA will increase from 4 to 12 percent during the next three years. Thus, in the future, a typical following aircraft should be of this weight category. In our studies, in parallel with the IL-103 aircraft, we consider the IL-114 (see Figure 5).

Boeing and Airbus agree that the fundamental tendency is the aircraft size growth, and at first it will take place in the middle class of aircraft. Growing sizes of aircraft result in increasing safe separation distances, which degrades the general effect of increasing airports' capacities. In this case the role of new technologies is to provide aircraft layouts, which make it possible to maintain previous safe separation distances for heavier aircraft.

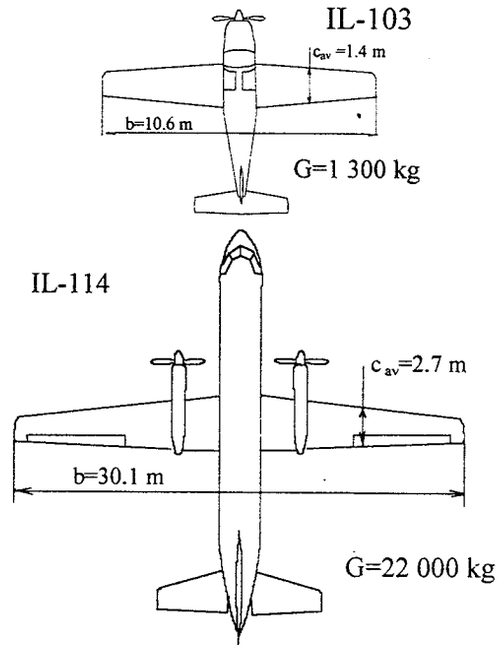

FIGURE 5 – Small and medium airplanes used in the investigations.

I. Vortex-wake model

A two-level vortex wake model, combining the asymptotically strict code **ZONWAKE** and the block engineering model **BEM**, was created[2]. This pivotal model is used in flight-dynamics and strength & aeroelasticity models.

The phenomenon under study involving the vortex-generating aircraft, the atmospheric turbulence, the pilot's actions, is stochastic in nature. We have at least two sources of stochasticity: pilot actions and atmospheric turbulence. Sources, types and scales of turbulence and environmental influences on the vortex wake evolution are discussed briefly in Ref. [6]. Generally speaking, the problem is beyond the frames of an initial-boundary-value problem for the Navier-Stokes equations. Up to now, the possibilities for chaotic bifurcation of these solutions are not proved. The aerodynamic wake-vortex model is deterministic. The element of stochasticity is introduced into the complete model by means of flight-dynamic **FDM** and structure & aeroelasticity **SAM** models.

I.1. ZONWAKE code

Zonal approach is based on the assumption that the problem considered has at least two significantly different scales. According to these scales, four zones are considered with proper equations and boundary conditions in each zone:

1. Aircraft near field where a panel method, which takes into account the rollup of the vortex sheets both from the trailing edge and side edges, is used.
2. 2D unsteady analogy for the far wake zone for vortex sheets calculations including sinuous instability effects based on Crow's solution with empirical corrections.

3. Euler equations in a narrow zone along the wake axis (inside zone 2).
4. Reynolds-averaged equations for an internal subzone (inside zone 3), where the anisotropic algebraic turbulence model is used.

Numerical matching on the zones boundaries are used to close the problem.

Presented in Figures 6-8 are the computed results of tangential velocity distribution, turbulent core radius and circulation for the A-3XX aircraft's[7] wake in cruise regime (V_∞=175 m/sec, α=5°, Γ_0=630 m^2/s) up to x=25km.

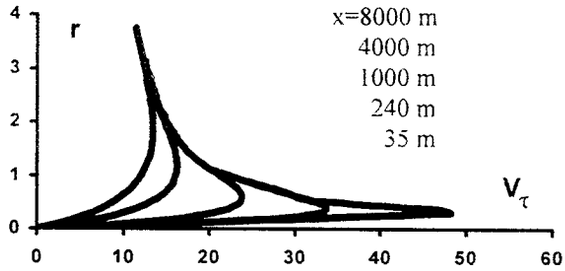

FIGURE 6 – Tangential velocity distribution.

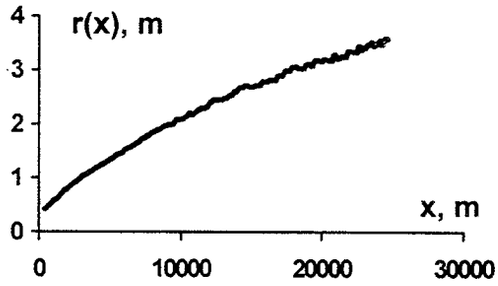

FIGURE 7 – Turbulent core radius.

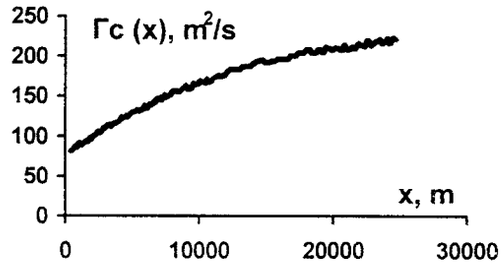

FIGURE 8 – Turbulent core circulation.

The growth of oscillation amplitudes and the rotation of oscillation planes as functions of distance from the wake generators (A-3XX and B-747) are presented in the Figures 9, 10. The same initial amplitude and flight parameters are used in both cases. The main difference from Crow's model[8] is the consideration of spatial vorticity distribution (that is more precisely accounting for the vortex generating aircraft). As a new result we have the rotation of the oscillation plane (see Figure 10). The most interesting from a practical standpoint is a slower growth of oscillation amplitude for the B-747 in comparison with the A-3XX.

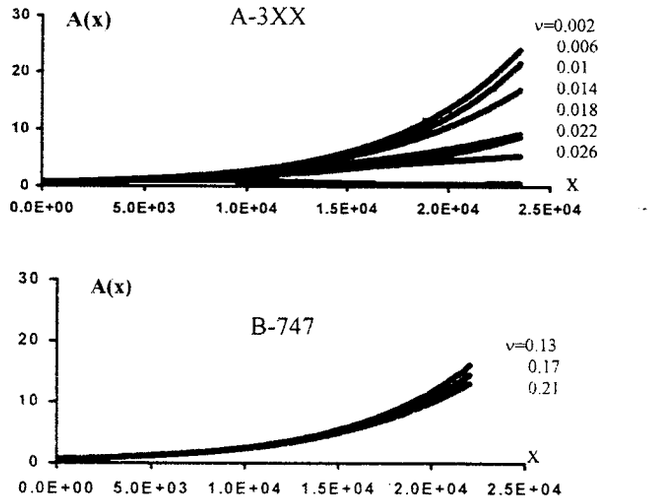

FIGURE 9 – Growth of oscillation amplitude.

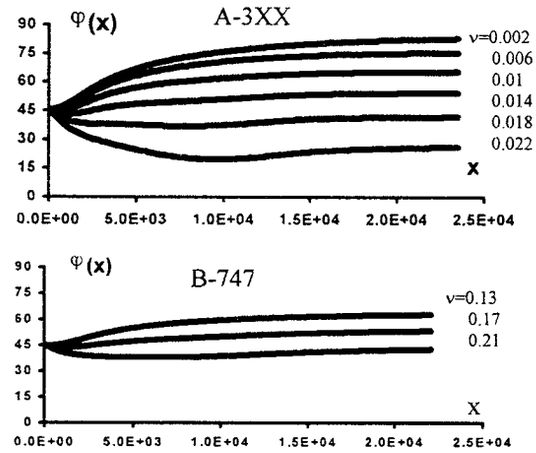

FIGURE 10 – Rotation of oscillation planes.

The amplitude of oscillation as a function of frequency at a distance of x=20 km for the A-3XX is presented in the Figure 11. Dashed line depicts the corresponding results for the B-747.

Presented in Figures 12, 13 are the pictures of the vortex wake in horizontal and cross-sectional planes for the last 7 km behind the A-3XX. The cross-link time t_{CL}=128.6 s (D_{CL}=22.5 km) can be used for safe separation distances estimation.

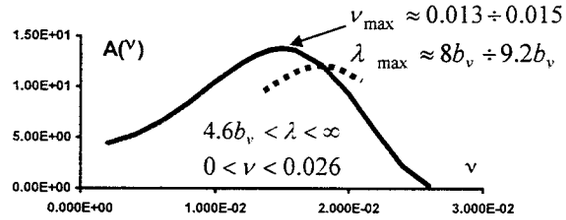

FIGURE 11 – Amplitude of oscillation as a function of frequency.

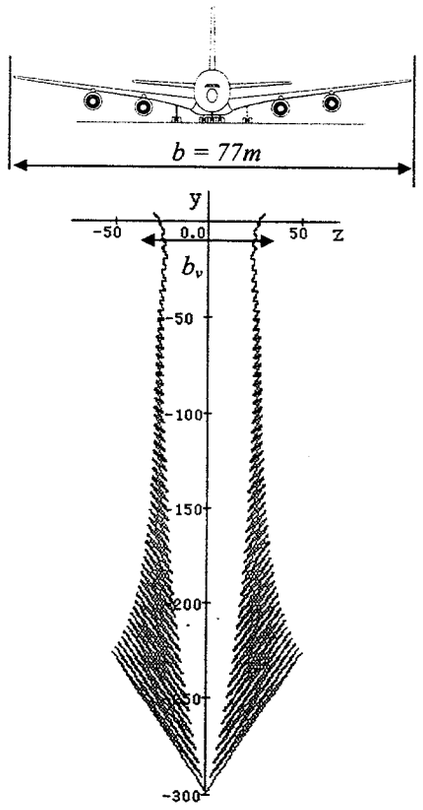

FIGURE 12 – Sinuous instability in a cross-sectional plane.

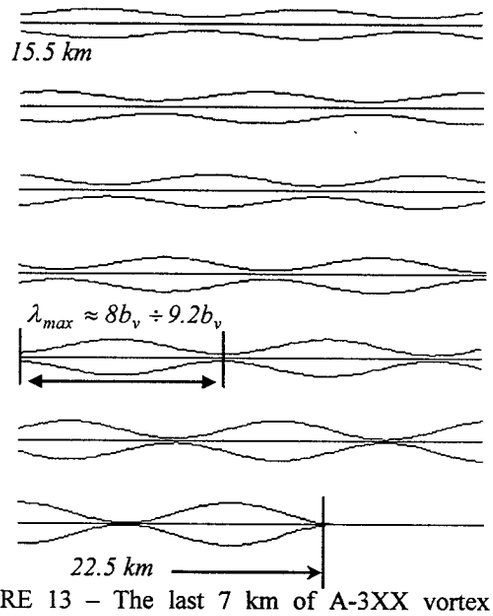

FIGURE 13 – The last 7 km of A-3XX vortex wake oscillation (V_∞=175 m/s, α=5°, Γ_0=630 m^2/s, A_0 = 1 m).

The results of comparison of the A-3XX and B-747 layouts for the same flight conditions and initial disturbances are presented in Table 1. Approximately the same cross-link time can be explained by the smaller amplitude growth rate for the B-747 and grater wing span for the A-3XX. However in accordance with modified empirical formulas[9]:

$$A_0(q) = \frac{b_{eq}}{2}\left(e^{-10} + e^{-1.6 \cdot V/q}\right);\ V=\Gamma/(2\pi b_v) \qquad (1)$$

$$b_{eq} = b_v \cdot 2h_v / \sqrt{b_v^2 + 4h_v^2}$$

the initial amplitudes at the same atmospheric turbulence and flight conditions for the A-3XX must be smaller (A_0= 1.25 m) than for the B-747 (A_0=2.18 m). In the last case the cross-link time (and in the first approximation the safe separation distance) for the A-3XX must be 25 s (that is for such speed - 2.4 nm) grater.

Aircraft	t_{CL}, s	D_{CL}, km	A_0, m
B-747	127.8	22.36	1
A-3XX	128.6	22.5	1
B-747	80.4	14.1	2.18
A-3XX	105.7	18.5	1.25

TABLE 1 - Cross-link time and distance (V_∞=175 m/s, q=1 m/s).

I.2. Block engineering model

The block engineering wake model[10] is an asymptotically not rigorous combination of experimental results, analytical investigations and CFD modeling and based on the published theoretical and experimental results. This model includes the basic physical phenomena of the wake flow:

1. Aircraft geometry effect (on the velocity distribution outside the turbulent core, on initial values of the turbulent core radius and circulation).
2. The multiple vortex structure of the wing with high-lift devices on vortex wake destruction.
3. Turbulent vortex core growth and circulation loss due to atmospheric turbulence.
4. The effect of atmospheric turbulence on the rate of vortex circulation loss and, as a consequence, the rate vortex core growth and vortex pair dynamics.
5. Atmospheric stratification effect.
6. Sinuous instability of the vortex pair as the main mechanism of vortex wake destruction (wake lifetime evaluation).
7. Ground proximity effect on the vortex wake dynamics, the rate of vortex circulation loss and, as a consequence, the growth of the turbulent core.

The methodology described above was used for computing the structure of the vortex sheet rolled up behind the B-747. When computing the spanwise circulation distribution in landing regime the following parameter values were used:

$$V_\infty=70\ m/s,\ \alpha_\infty=10^o,\ C_L=1.44,\ \delta_{flap}=30^o,$$
$$S=511\ m^2,\ b=58.6\ m,\ b_v=42\ m,\ c_{av}=8.7\ m, \qquad (2)$$
$$c_{tip}=4.1\ m,\ \Gamma_o=593\ m^2/s.$$

Figures 14-19 demonstrate time variations of the wake height above the ground and vortex circulation losses for various initial heights with taking into account circulation losses and ground proximity and without taking into account atmospheric stratification. Thus estimated the wake lifetime is t_{CL}=67 s at q=1 m/s.

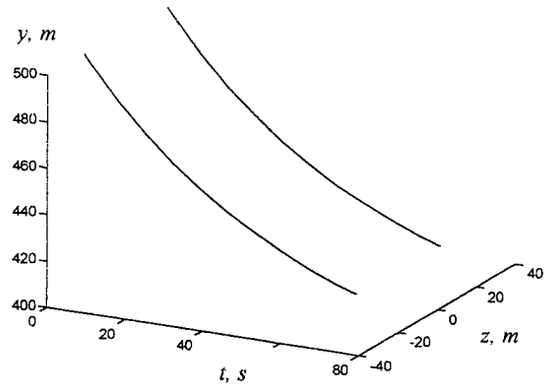

FIGURE 14 – Vortex pair descent from $h_0=500\ m$.

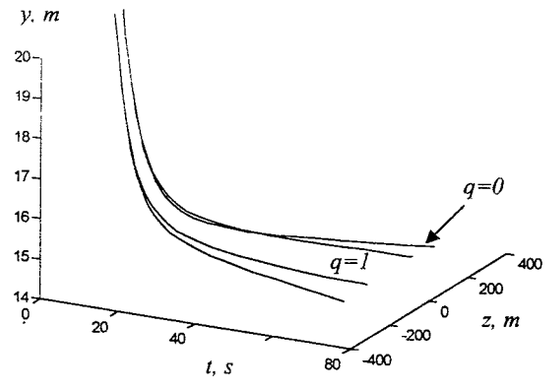

FIGURE 15 –Vortex pair descent from $h_0=20\ m$ for two values of atmospheric turbulence.

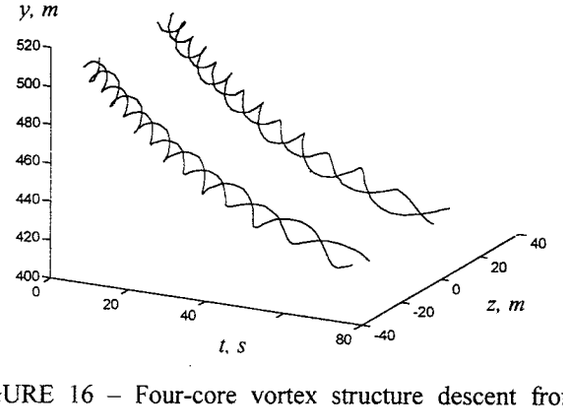

FIGURE 16 – Four-core vortex structure descent from $h_0=500\ m$.

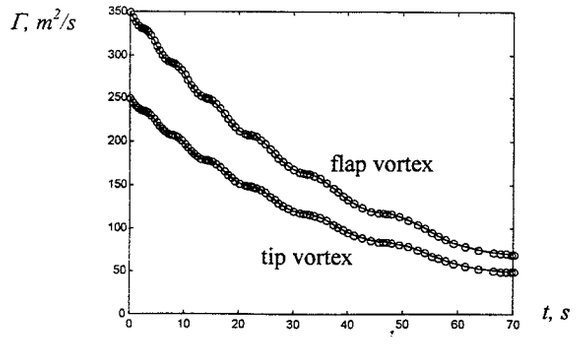

FIGURE 17 – Circulation variation during the descend of the four-core structure from $h_0=500\ m$.

The height of vortex pair descent due to circulation losses is $\Delta y<80\ m$. At low altitudes circulation losses become greater (see Figures 17, 19), hence the vortex pair behavior in the turbulent atmosphere differs significantly from that without turbulence. In the case of four-core structure the circulation loss effect is more pronounced because it changes the rate of vortices rotation about its centroid.

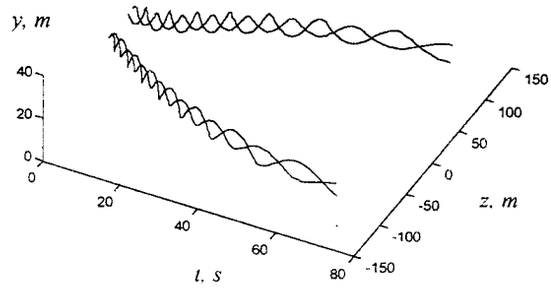

FIGURE 18 – Four-core vortex structure descent from $h_0=20\ m$.

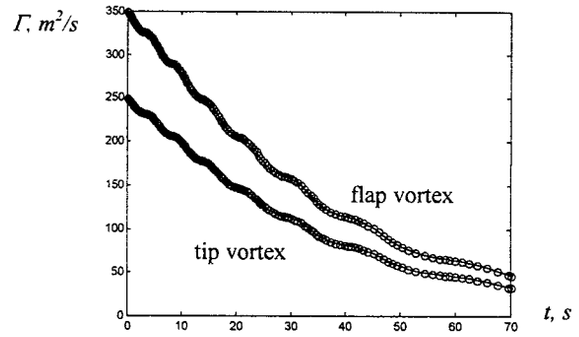

FIGURE 19 – Circulation variation during the descend of the four-core structure from $h_0=20\ m$.

Figure 20 shows the results of computing the development of the symmetrical mode of sinusoidal disturbances for the two-core structure. The initial disturbance was specified at $t=0$ in the plane inclined at an angle of $\varphi=45^o$ to the horizontal plane and the amplitude A_0 was taken according to empirical formula (1). Problem parameters correspond to the landing regime for the B-747 (2) and the disturbance wavelength to the mode which grows most rapidly (to the linear approximation), $\lambda_{max}=9b_v$. It should be noted that to the nonlinear approximation the λ_{max} is smaller.

Computations have shown that the amplitude of disturbance grows quicker for the internal halfwave than for the external one. Because of this the wake lifetime $t_{CL}=66\ s$ is less than that in the linear approximation and is in close agreement with the value $t_{CL}=67\ s$ observed experimentally[11]. In the case of calm atmosphere $q=0$ computation yields $t_{CL}=202\ s$ ($t_{CL}=187\ s$ experimentally).

Similar computations for the four-core structure ($\lambda=9b_v$, $\Gamma_{flap}=350\ m^2/s$, $\Gamma_{tip}=250\ m^2/s$, $z_{flap}=15\ m$, $z_{tip}=23m$, $r_{flap}=r_{tip}=1\ m$, $q=1\ m/s$) yield $t_{CL}=60\ s$. In the case of $q=0$ $t_{CL}=160\ s$, which is substantially less than for the two-core model. The decrease of the wake lifetime is

explained by the excitation of sinusoidal oscillations produced by the rotational motion of the vortex pair about its centroid (see Figures 21, 22).

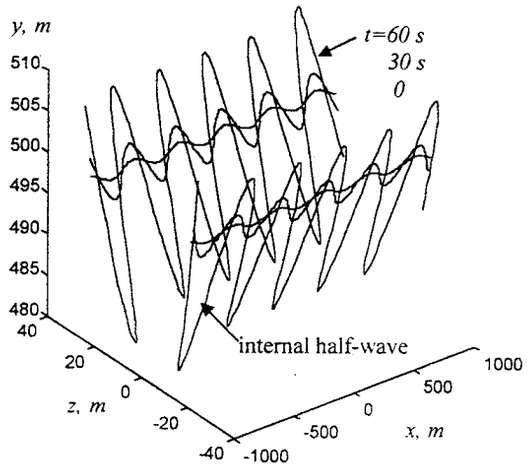

FIGURE 20 – Sinuous instability development for the vortex pair ($q=1$ *m/s*, $r_o=2$ *m*).

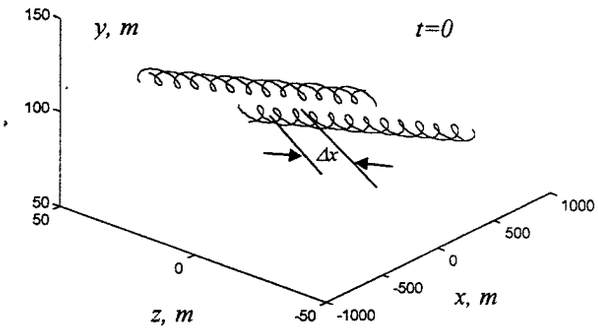

FIGURE 21 – Sinuous instability development for the four-core structure (the spatial step of the vortex pair $\Delta x=315$ *m* approaches to $\lambda_{max}=360$ *m*).

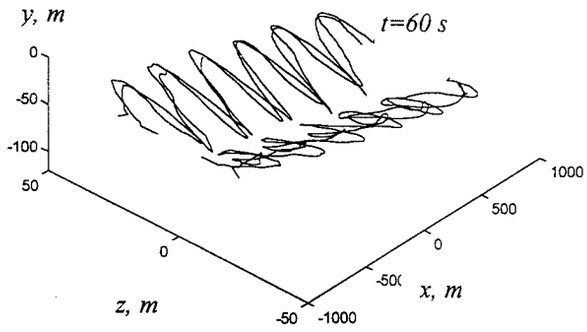

FIGURE 22 – Effect of synchronization and vortices cores margin with subsequent two-core vortex structure formation.

Parametric investigations have shown that for the four-core structure the minimum lifetime is realized with shorter wavelengths ($\lambda_{max}=7b_v$) and is $t_{CL}=145$ *s* at $q=0$ and $t_{CL}=52$ *s* at $q=1$. This effect is caused by the additional influence of the rotation of the vortex cores relative each other on the development of sinuous instability.

Thus, lowering high-lift devices in takeoff and landing regimes can be favorable for shortening vortex wake lifetime. In this connection a problem can be posed on the selection of a flap deflection optimum from the standpoint of reducing safe-separation distances between aircraft.

II. Flight-dynamic model

The main goal of the investigations in creation of the flight-dynamic model[12] (**FDM**) is the evaluation of safe distances between aircraft landing on the same runway. The «worst case» approach to the solution of this problem is non-constructive because it leads to excessive enlargement of allowable distances. Instead, the probabilistic approach seems to be more realistic. By using this model the probability of dangerous wake encounters can be calculated depending on the distance between aircraft and aircraft parameters (see Figure 23). Realistic values of flight incident probability can be derived using the modified Monte-Carlo procedure.

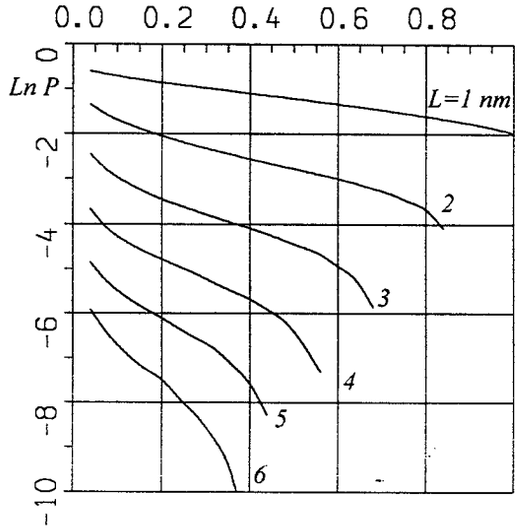

FIGURE 23 – Probability P of exceeding the critical value of rolling moment for different distances between aircraft (B-747 and Tu-154, flying the glide slope).

The model takes into account: the movement of vortices near the ground, circulation distribution and dissipation, as well as unstable oscillations of the vortices. The wind model includes two components of the steady wind and turbulent gusts:

$$U_x(h) = u_x(0.53 + 0.47 \lg h),$$

$$U_z(h) = u_z(0.53 + 0.47 \lg h)$$

were u_x and u_z are independent Gaussian stochastic quantities

$$\bar{u}_x = -2.7 \text{ m/s}, \quad \bar{u}_z = 0, \quad \sigma_{ux} = \sigma_{uz} = 3.75 \text{ m/s}.$$

The longitudinal u, lateral w and vertical v components of the turbulent wind gusts represent uncorrelated Gaussian random processes with the parameters:

$$\sigma_u = \sigma_z = 0.18\,\tilde{u}, \quad \sigma_y = 0.09\,\tilde{u},$$
$$L_u = L_w = 180\ m, \quad L_v = h,$$

where $\tilde{u} = (u_x^2 + u_z^2)^{1/2}$ is the magnitude of the wind at a height of *10 m*. The spectral density considered for the turbulent gust components corresponds to the von Karman model (the Dryden model may be used too).

The methodology of statistical modeling for obtaining the probability of large deviations of aircraft trajectory kinematic parameters has been developed[13].

It is interesting that the *Crow instability*, despite being the main form of vortex wake destruction, may increase the time interval of aircraft - vortex interaction, and from this standpoint increase safe separation distance between aircraft.

The results of calculations for 200 realizations are shown in Figure 24 on a plane of wind velocity components. The asterisks mark adverse realizations (lateral deviation *z>21 m*), circles - all others.

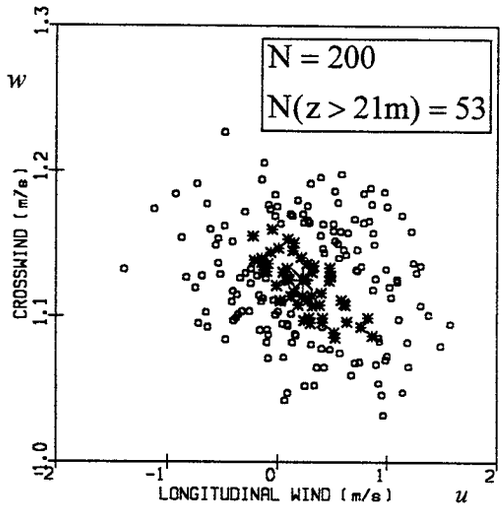

FIGURE 24 – Methodology of statistical modeling (G_1=*135 t*, G_2=*50 t*, Δx=*3 nm*).

The allowable distances Δx are determined in Figure 25 both with vortex deformation (dashed line) and without vortex deformation (solid line). As can be seen, the deformations of the vortices are more essential for aircraft with large weight and correspondingly large wingspan. From these results it also follows that the weight category of "medium" aircraft, according to ICAO norms is too "wide" - allowable distances between aircraft in various pairs in this category can differ by 3 miles. The US regulations are more realistic.

In the right diagram of Figure 25 the dependence of allowable rolling moment induced by vortices

$$\bar{f} = \frac{\Delta C_l}{\Delta C_{l_{max}}(\delta_{ail})},$$

on weight of the following aircraft is shown. The substantial increase of the parameter $\bar{f}$ for small-weight airplanes in statistical simulations[13], is connected first of all with the reduction of time of influence of a vortex on the aircraft with small wingspan.

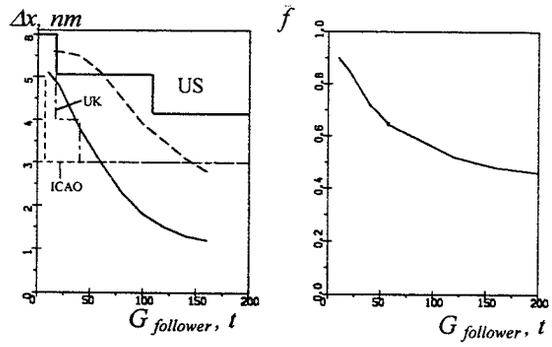

FIGURE 25 – Allowable distance behind heavy leader aircraft: using the criterion $P(z > 21\,m) = 10^{-5}$.

III. Strength & Aeroelasticity model

The main problem in creation of the strength & aeroelasticity model[14] (**SAM**) is to develop the criteria for choosing safe separation distances between aircraft from the structure and aeroelasticity standpoint. The critical situation in this case is the cross-track wake encounters.

Experimental simulation in a low-speed wind tunnel with the gust simulator and fixed and free flying Froude-similar models are used for testing the mathematical model developed[15].

Figure 26 shows the time history of the maximum wing root bending moment ΔM. Here Δt is the time interval between B-747 flight and IL-103 aircraft cross wake penetration. The safe time interval can be found as the time of reaching the limit load. At standard turbulence level Δt=*45 s*, whereas at a very weak turbulence it reaches *165 s*. That is, for a flight speed of *78 m/s* we have safe distances Δx=*3510 m* and Δx=*12870 m*, respectively. For comparison, according to the US regulations it should be Δx=*6 nm* (*11100 m*) for such pair of aircraft (see Table 2).

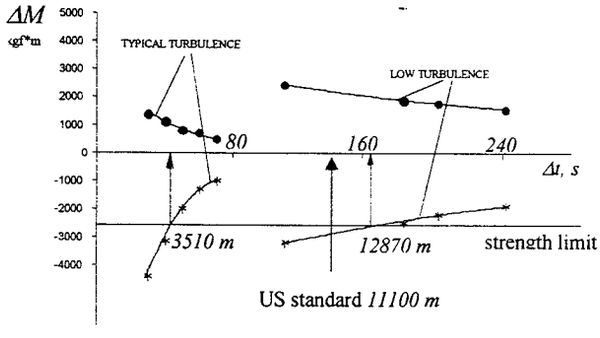

FIGURE 26 – Loads as a function of time (IL-103 aircraft cross wake penetration behind the B-747).

Heavy	$G > 115.7\ t$
Medium	$18.8\ t < G < 115.7\ t$
Small	$G < 18.5\ t$

Table 2 Weight categories in the US regulations.

In accordance with the new US regulations a safe separation behind heavy aircraft is equal to Δx=*5 nm* for

medium aircraft and $\Delta x=6$ *nm* for small ones. Dividing these distances by the wake-generator speed one can obtain the safe separation intervals $t_{sf}=133$ *s* for the IL-114 and *159 s* for the IL-103. By taking into account the random character of atmospheric turbulence with the distribution density:

$$\varphi(q)=\sqrt{\frac{2}{\pi}}\frac{1}{\sigma}exp\left(-\frac{1}{2}\frac{q^2}{\sigma^2}\right) \qquad (3)$$

for fine weather	$\sigma = 1$ *m/s*
for cloudy weather	$\sigma = 2.1$ *m/s*
for storm weather	$\sigma = 3.5$ *m/s*

by means of statistical modeling[14] (formula (3) accepted for atmospheric turbulence was incorporated into the deterministic **BEM**, which allows stochastic elements to be introduced to wake parameters) the probabilities P of safely executing vortex-wake crossing in the case of fine weather conditions were obtained (see Table 3). The worst case of vortex core encounter is considered. But the vertical distance can also be considered as a random variable, which will increase the probability of safe wake encounter. Nevertheless, in both cases, the new regulations do not guarantee that wake intersection is safe from the structural strength standpoint.

Follower aircraft	V_∞ *m/s*	t_{sb} *s*	P
Medium	65	133	0.871
Medium	128	133	0.761
Small	36	159	0.943
Small	78	159	0.683

TABLE 3 - Probability of safely executing vortex-wake crossing after the Heavy leader for standard safe separation intervals.

So a safety zone round an aircraft can be constructed[16]. The example of such indicator diagram is represented in Figure 27. For small intersection angles close to parallel flight the safe distances are defined by stability and controllability of an aircraft, encountering the vortex wake, whereas at large encounter angles the safety zone will be limited by aircraft strength.

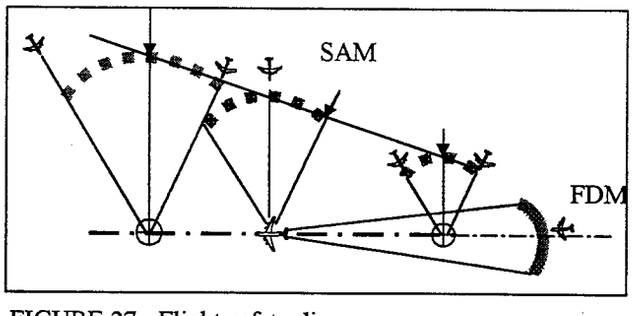

FIGURE 27 - Flight-safety diagram.

Using this algorithm the Ground-based and Onboard system of drawing Vortex Flight Safety Diagram (**GOVFSD**) can be created. It is an integrated computer code for construction of an indicator diagram of safe separation distances for an aircraft following a wake generating aircraft with allowance for wake dissipation by atmospheric turbulence and for restrictions on the flight dynamics and the structural strength of a given aircraft, which can find itself in a vortex wake.

Conclusions

One of the main results obtained is the creation of the two-level wake-vortex model which includes the asymptotically rigorous single wake model **ZONWAKE** constructed on the basis of dividing the problem domain into a set of subdomains and the block engineering model **BEM** based on the asymptotically non-rigorous combination of test data and the results of numerical simulation. This model is the pivotal one which is used in flight-dynamics **FDM** and strength & aeroelasticity **SAM** models, and combines them in a single structure.

On the basis of the developed mathematical models and experimental methodology, the effectiveness was assessed of the possible measures and technical decisions aimed at improving flight safety and reducing safe-separation distances between aircraft when flying along the glide path.

The creation the safety zone diagram (Figure 27) is only the first step. The next steps are:

1. Jet-vortex wake visualization in VFR landing approach using microparticles[17] and molecular clusters. For these purpose the following problems must be solved: choice of the spectral range of activity of the simplest-composition clusters, investigations on the possibilities for minimizing the power required of the scanning EM radiation and optimizing the receivers, working out the concepts of airborne and ground-based systems for vortex wake detection.
2. Creation of the Onboard early Vortex Detection and vortex Avoidance maneuver System (**OVDAS**) using standard on-board sensors[18]. This is an algorithm and computer code for the creation of an onboard system (compatible with the TCAS) for early detection of vortex wakes, construction of the best algorithm for avoiding a wake with the parallel indication of a proposed maneuver on a display.
3. Measures on improving the controllability and survivability of wake-encountering aircraft (use of the wing control surfaces to increase the available roll and yaw control authority, automatic dynamic load alleviation systems in cross-track wake penetration). The results obtained[19] have shown that the use of aerodynamic surfaces (flaps, spoilers) allows changing the wing lift and producing additional rolling moments of $\Delta C_l=0.05$-0.06 that are comparable to those of the outboard ailerons while retaining a satisfactory level of aircraft aerodynamic characteristics in takeoff and landing flight regimes. So, there is a possibility of doubling the available roll control power using differential and asymmetric flap and spoiler deflections without degrading aircraft

takeoff and landing characteristics. Favorable to this is also the development and use of the Onboard early Vortex Detection and Increase Aircraft Survivability warning System (**OVDIASS**) to make crews capable of bringing into operation additional roll control devices in proper time.

4. Finding the means of artificial vortex-wake aging and layouts optimum from the wake hazard standpoint. Considered as a means of acting upon the vortex wake are the *wing high-lift devices* and *aircraft engines*. Artificial aging of the vortex wake can be accomplished with engine jets affecting its formation. The investigations in this case are aimed at finding appropriate engine layout and mode of operation. When creating new ultra-heavy aircraft and the aircraft of all-new class (supersonic, "flying-wing", etc.), the aerodynamic configuration and, especially, the layout of the high-lift wing for the landing flight regime should be chosen with regard to the possibilities to shorten safe-separation distances.
5. The use of *flight simulators* with the aim of investigating the control and stability of the encounter aircraft, evaluation of possible technical decisions, determining the safe-separation criteria, elaborating the pilot's skill to cope with hazardous situations.

Acknowledgments

This paper is a brief presentation of the results obtained by the team of TsAGI's researchers in the course of implementing the Projects VORSAF "Investigation of Vortex Wake Evolution and Flight Safety Problems" and "Flight Safety, Aircraft Vortex Wake and Airport Operation Capacity" financed by the International Science and Technology Center (Grants #201-95, #1018-98). The creation of this research team striving to solve this problem is also a result of great importance.

The author wishes to acknowledge Profs. V.A. Yaroshevsky, O.A. Kuznetsov, A.L. Stasenko, Drs. A.M. Gaifullin, V.E. Gryazin, V.P. Kuzmin, Yu. S. Mikhailov, R.I. Osminin, G.G. Soudakov for numerical results and useful discussions of the work.

References

1. Safety Issues Related to Wake Vortex Encounters During Visual Approach to Landing. National Transportation Safety Board. Special Investigation Report *NTSB/SIR–94/01*, 1994, 95 p. Washington, D.C. 20594.
2. Vyshinsky, V.V., Soudakov, G.G. Investigation of the vortex wake evolution and flight safety. *ICAS-96-1.11.3*, pp. 2590-2600.
3. Bobylev, A.V., Kuzmin, V.P., Yaroshevsky, V.A. An analysis of stochastic effects of the vortex wake on aircraft motion at automatic landing. *Trudy TsAGI*, Vol. 2622, 1996, pp. 197-208, in Russian.
4. Mulally, A. «Aerospace and global working together», *World Aviation Congress*, October 15, 1997.
5. Butterworth-Hayes, Ph. The benefits of thinking small. *Aerospace america*, July 1997, pp. 4-5.
6. Spalart, P.R. Airplane trailing vortices. *Annu. Rev. Fluid Mech*, 1998, Vol. 30, pp. 107-138.
7. Greff, E. Aerodynamic design and technology concepts for a new ultra-high capacity aircraft. *ICAS-96-4.6.3*, pp. 1321-1337.
8. Crow, S.C. Stability Theory for a Pair of Trailing Vortices. *AIAA Journal*, 1970, No. 12, pp. 2172-2179.
9. Stuever, R.A., Greene, G.C. An Analysis of Relative Wake-Vortex Hazards for Typical Transport Aircraft. *AIAA Paper* 940810, 1994, 15 p.
10. Vyshinsky, V.V., Soudakov, G.G. Vortex wake and a plane. "Aviation-2000. Prospects", pp. 131-138. *International Symposium Proceedings*, Zhukovsky, Russia, August 19-24, 1997.
11. Greene, G.G. An approximate model of vortex decay in the atmosphere. *J. Aircraft*, Vol. 23, No. 7.
12. Bobylev, A.V., Kuzmin, V.P., Yaroshevsky, V.A. Mathematical simulation of the wake vortices effect on aircraft motion during automatic landing. *Trudy TsAGI*, Vol. 2627, 1997, pp. 198-208.
13. Kuzmin, V.P. Estimation of wake-vortex separation distances for approaching aircraft. "Aviation-2000. Prospects", pp. 267-274. *International Symposium Proceedings*, Zhukovsky, Russia, August 19-24, 1997.
14. Kuznetsov, O.A., Orlova, T.I., Chizhov, V.M. Evaluation of safe-separation distances between aircraft from the strength standpoint. *Trudy TsAGI*, Vol. 2627, 1997, pp. 138-147.
15. Kuznetsov, O.A., Osminin, R.I. Wind tunnel investigation of an aircraft dynamic loads due to vortex gusts. *Trudy TsAGI*, Vol. 2627, 1997, pp. 157-168.
16. Kuznetsov, O.A., Orlova, T.I., Osminin, R.I. Aircraft dynamic loads at vortex wake encounter. "Aviation-2000. Prospects", pp. 377-382. *International Symposium Proceedings*, Zhukovsky, Russia, August 19-24, 1997.
17. Grinats, E.S., Kashevarov, A.V., Stasenko, A.L. Gasdynamics and optics of an aircraft condensable wake. *SAE* 96-5548, 1996.
18. Gryazin, V.E. Algorithms of vortex wake detection and flight-director control for executing wake-avoidance maneuvers. "Aviation-2000. Prospects", pp. 139-146. *International Symposium Proceedings*, Zhukovsky, Russia, August 19-24, 1997.
19. Mikhailov, Yu. S. Simulation of vortex wake impact on a general-aviation aircraft in a wind tunnel using the airfoil lattice. *SAE* 96-5545, 1996.